SSRG International Journal of Electrical and Electronics Engineering
ISSN: 2348-8379/https://doi.org/10.14445/23488379/IJEEE-V11I9P123

Volume 11 Issue 9, 250-260, September 2024

Original Article

A Low-Rating Renewable Sources Power Sharing to the Grid Using Space Vector Operated Switched Capacitor Multilevel Inverter and Fuzzy Integrated Switched Z-Source Converter

Sapavath Sreenu[1,2], J. Upendar[3]

[1]*Department of Electrical Engineering, Keshav Memorial Institute of Technology, Hyderabad, Telangana, India.*
[2,3]*Department of Electrical Engineering, University College of Engineering, Osmania University, Hyderabad, Telangana, India.*

[1]*Corresponding Author : sreenu06274@gmail.com*

Received: 11 July 2024 Revised: 13 August 2024 Accepted: 10 September 2024 Published: 28 September 2024

Abstract - *Renewable energy power sharing with the grid presents various challenges and issues in maintaining power quality. Complications are reduced for higher-rated renewable sources compared to lower-rated sources. Higher-rated sources have higher voltages, making it less complex to convert and share power with the grid. However, for sources with voltages in the range of 20-30V, sharing power with voltage gains is a challenge. In this paper, an SZSC is introduced at the DC link of the combined renewable sources. This SZSC boosts the voltage at the DC link to 3-4 times the original voltage as needed. The voltage at the output of the SZSC is regulated by an FIS voltage controller to improve voltage stability and magnitude generation compared to conventional PI regulators. The boosted DC voltage is then fed to a three-phase SC-MLI operating in synchronization with the grid's three-phase voltages. To reduce harmonic generation, the 9-level SC-MLI uses the SV-PWM technique with signals generated according to the section selection table. For analysis, the renewable sources considered are solar panels and a wind farm supported by a battery module. All these sources and storage units are individually controlled by MPPTs and voltage controllers to ensure stable DC link voltage generation. Power balancing data, voltage stability analysis, and harmonic analysis are performed using MATLAB Simulink software and the Electrical toolbox.*

Keywords - *Switched Z-Source Converter (SZSC), Fuzzy Inference System (FIS), Proportional Integral (PI), Switched Capacitor Multi-Level Inverter (SC-MLI), Space Vector Pulse Width Modulation (SV-PWM), Maximum Power Point Tracking (MPPT), MATLAB Simulink.*

1. Introduction

Renewable sources such as solar, wind, hydro, and geothermal power produce energy with minimal impact on the environment compared to fossil fuels. They help mitigate climate change by reducing greenhouse gas emissions and other pollutants that contribute to air and water pollution. Unlike finite fossil fuels, renewable sources are inexhaustible and widely distributed globally [1]. This reduces dependence on imported fuels and enhances energy security for nations, promoting stability and resilience in energy supply. Investing in renewable energy creates jobs in manufacturing, installation, maintenance, and research. It fosters economic growth by stimulating innovation and technological advancement in energy production and storage. By reducing air and water pollution, renewable energy sources contribute to improved public health outcomes. This is particularly significant in urban areas where fossil fuel combustion contributes to respiratory diseases and other health issues.

Renewable energy sources have minimal operating costs once installed, unlike fossil fuels, which are subject to price fluctuations and geopolitical uncertainties [2]. This stability can benefit consumers and businesses alike by providing predictable energy costs over the long term. Renewable energy projects often provide opportunities for rural and economically disadvantaged communities. They can offer new income sources through land leases for wind and solar farms or by hosting hydroelectric projects, thereby revitalizing local economies. The development of renewable energy technologies drives innovation in energy storage, grid management, and efficiency improvements [3]. This, in turn, benefits other sectors and helps create a more sustainable energy infrastructure. Renewable energy plays a crucial role

in reducing the carbon footprint of human activities. As countries strive to meet international climate commitments and targets, renewable energy is indispensable in achieving significant reductions in greenhouse gas emissions [4].

For lower rating applications, the renewable source voltage levels are very low, which need to be boosted up to high voltage magnitude using power electronic devices. In conventional methods converters like DC-DC boost converter or Quasi-Z Source Inverter (Q-ZSI) are used for voltage boosting [5]. A Q-ZSI is a power conversion topology that enhances the traditional Voltage-Source Inverter (VSI) and Current-Source Inverter (CSI). It is part of the broader category of Z-Source Inverters (ZSI), which were developed to address the limitations of conventional inverters. Unlike traditional inverters, which require separate boost and inverter stages, qZSI combines both functions in a single-stage conversion process. This makes the design more efficient and compact. A key innovation in qZSI is the ability to tolerate a "shoot-through" state, where both switches in the same leg of the inverter are turned on simultaneously. In conventional inverters, this would lead to a short circuit and potential damage. In qZSI, this state is actually beneficial and used to boost the input voltage, improving performance and reliability.

However, these converters have very less voltage gain and high harmonic content. For higher voltage gain and reduced harmonic voltages, SZSC and SC-MLI are used, respectively [6]. The SZSC can boost the DC voltage up to 5 times, and SC-MLI creates multi-level AC voltage with reduced harmonic content.

A SC-MLI is a type of power inverter that uses switched capacitors to achieve voltage boosting and multilevel output waveforms without the need for inductors or a large number of isolated DC sources, which are common in traditional multilevel inverter topologies like the cascaded H-bridge inverter. The SC technique uses capacitors charged to specific voltages and switches to dynamically alter the configuration of these capacitors. By switching the capacitors in series or parallel, the inverter generates different voltage levels.

For the analysis, the input sources considered are PV panels, wind turbine generators and battery storage modules. Maximum PV panel power is extracted, and the wind turbine generator uses MPPTs. The battery storage module is a support to the renewable sources for DC voltage stability. The proposed system's complete structure with renewable sources, SZSC and SC-MLI is presented in Figure 1.

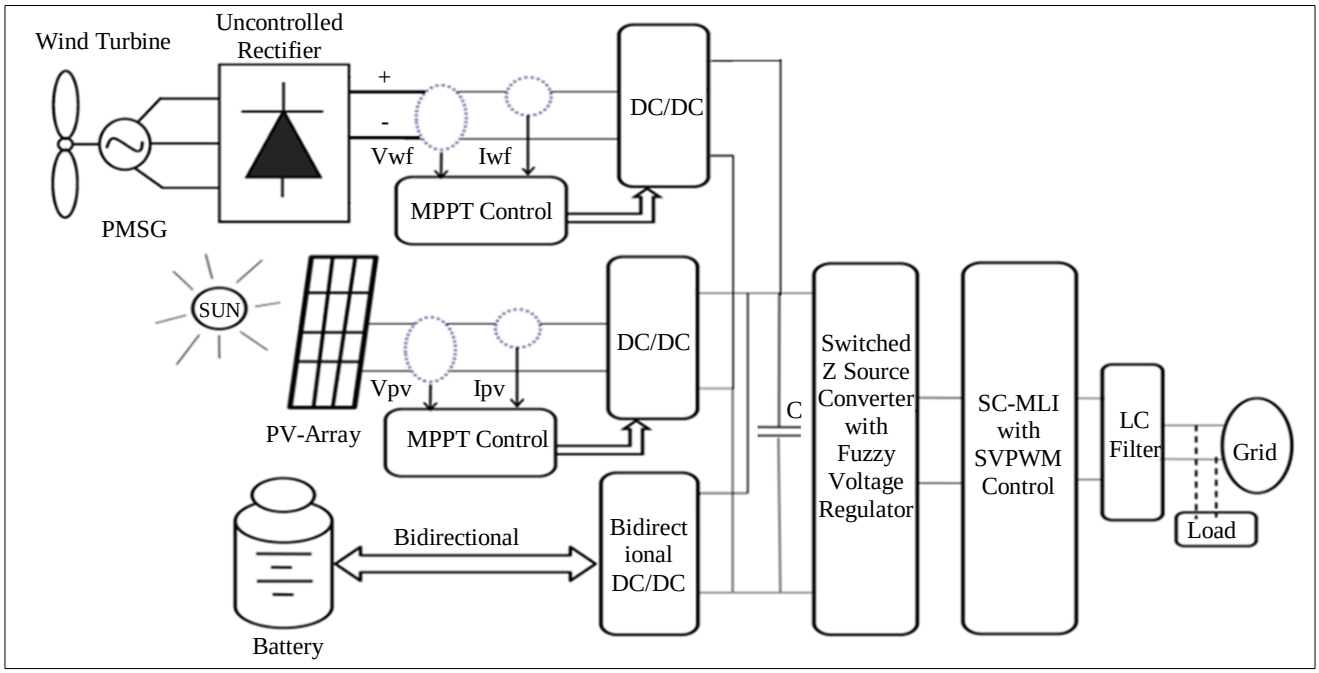

Fig. 1 Structure of renewable sources, SZSC and 3phase SC-MLI with SVPWM

As observed in Figure 1, all the source and storage modules are connected in parallel at the DC bus for power sharing. The PV panels and wind turbine generator are connected to unidirectional converters, whereas the energy storage module is connected to a bidirectional converter. The PV panels are connected to a 'DC-DC boost converter' operated with the Perturb and Observe (P&O) MPPT algorithm [7]. The wind turbine generator is integrated with Permanent Magnet Synchronous Generator (P&O) connected to a rectifier and 'DC-DC buck-boost converter' operated with the Power Signal Feedback (PSF) MPPT' algorithm.

The energy storage battery module is connected to a 'DC-DC bidirectional converter' for the exchange of power as per the availability of renewable sources. At the DC bus output, an SZSC topology is connected for boosting of DC bus voltage [8, 9]. For smother and stable control of SZSC a FIS voltage regulator is adopted for controlling the switch of the SZSC [10]. After boosting the DC bus voltage at the SZSC output terminals, a three-phase SC-MLI is connected to generate three phase 9-level PWM AC voltages. The SC-MLI is connected to the grid and loaded in parallel through the LC filter for Sin AC voltage generation. The SC-MLI is operated in synchronization with the three phase grid voltages using the SV-PWM technique for mitigation of harmonics and voltage stability.

2. Switched Impedance Source Converter

The SZSC is known for its flexibility in handling wide input voltage ranges and for its ability to regulate output voltages even when input voltages vary widely. Unlike traditional converters, which use capacitors and inductors in their filtering and energy storage networks, the SZSC uses a unique "Z-source" network. This network consists of an impedance network (often using a network of passive components like inductors and capacitors) that enables boost capability. One of the main advantages of the SZSC is its ability to perform bidirectional voltage conversion [11].

It can boost or buck the voltage without the need for additional stages or components typically required in conventional converters. These converters are particularly useful in applications where there is a need for high voltage gain, bidirectional power flow or where traditional converters may not efficiently handle wide input voltage ranges. Control techniques for switched Z-source converters include various modulation strategies to control the switching of the semiconductor devices effectively [12]. These techniques ensure efficient operation and desired output characteristics. A typical SZSC is presented in Figure 2 with one controllable MOSFET switch.

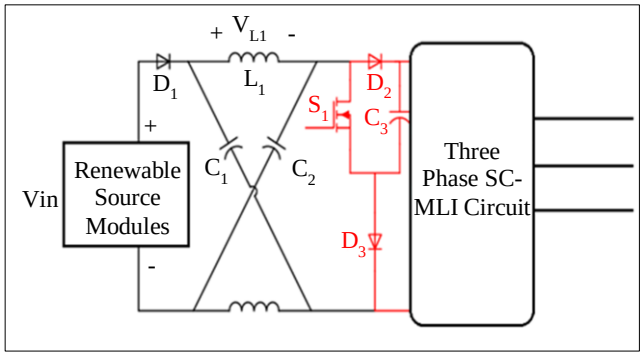

Fig. 2 Proposed SZSC topology

As per Figure 2, the passive elements C_1C_2 and L_1L_2 are connected in the Z network for voltage boosting and ripple reduction. The input diode D1 blocks reverse currents to the renewable source modules [13]. The MOSFET switch S1 is triggered using a PWM pulse generated by a voltage regulator. When switch S_1 is turned ON, inductors L_1 L_2 and capacitors C_1 C_2 store charge from the renewable source modules. During this time, the output capacitance C3 provides power to the SC-MLI, keeping the diode D_2 in reverse bias. During the switch ON time, the diode D_3 is forward biased, receiving current from S1.

When the S1 MOSFET is turned OFF, the charge in L1 L2 and C1 C2 discharge along with the renewable source modules in series. During the OFF state of S1, the C3 is charged through D2 also providing boosted voltage to the inverter. The output voltage (Vo) of the converter as per the inductor voltages is expressed as:

$$V_o = V_{in} + V_{L1} + V_{L2} \quad (1)$$

Both capacitors C1 and C2 ensure stable voltages on the input and output terminals with reduced ripple. The passive elements for the given topology are calculated as follows:

$$L_1 = L_2 = \frac{2V_i D(1-D)}{\%\Delta I_L i_o f_s} \quad (2)$$

$$C_1 = C_2 = \frac{i_o D}{\%\Delta V_C V_i (1-2D)} \quad (3)$$

Here, 'f_s' is the carrier frequency of S1.$\%\Delta I_L$ and $\%\Delta V_C$ are the % current ripple and % voltage ripple tolerated by the inductor and capacitor, respectively.

As per the given requirement, the SZSC elements are updated, generating boosted voltage at the output. The DC voltage (Vdc) at the output of the SZSC is calculated as per the duty ratio (D) of the switch S1 given as:

$$V_{dc} = \frac{1}{(1-4D)} V_{in} \quad (4)$$

Here, the duty ratio (D) of switch S1 is controlled by a voltage controller with a reference voltage (V_dc^*) given as per the requirement of the SC-MLI. The design of the voltage controller of the SZSC is presented in Figure 3.

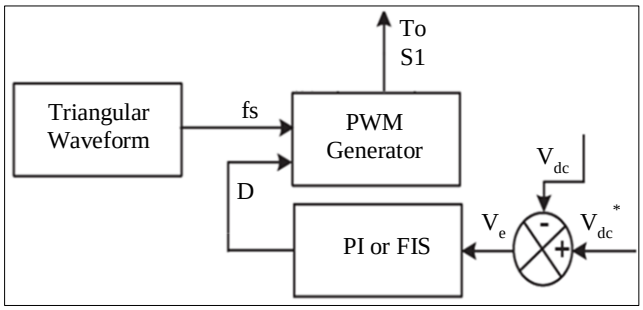

Fig. 3 Voltage controller for SZSC

The voltage controller has a voltage regulator, preferably a PI controller, which calculates the required duty ratio (D) expressed as [14]:

$$D = \left(K_p + \frac{Ki}{s}\right)(V_{dc}^{*} - V_{dc}) \quad (5)$$

Here, the 'proportional and integral gains' of the PI controller are tuned based on the output voltage response of SZSC. The duty ratio (D) signal is compared to a high-frequency triangular wave to generate pulses for switch S1. For better control over the output DC voltage with increased accuracy and reduced ripple, the PI regulator is replaced with a FIS voltage regulator [15].

The FIS tool has two inputs and one output, which are preferably error, change in error and duty ratio, respectively. The error (e) signal is generated by comparison of V_dc^* and V_dc, and the change in error (ce) is generated by comparison of the present value of 'e' (e(k)) and the previous value of 'e' (e(k-1)). The input signals are given as:

$$e = V_{dc}^{*} - V_{dc}$$

$$ce = e(k) - e(k-1) \quad (6)$$

Each variable is set with seven Membership Functions (MFs) specified with names taken as Very Big Negative (VBN), Big Negative (BN), Small Negative (SN), Zero (Z), Small Positive (SP), Big Positive (BP), Very Big Positive (VBP)'. The structures of these MFs regions of all variables are presented in Figure 4.

The input 'e' range is set between -100 to 100 as the reference voltage is considered at 100V for the generation of output voltage. The 'ce' range is set between -1 to 1 as the value does not exceed this range. The output 'D' range is varied as per the response of the output voltage of SZSC. The final range is set between -0.9 to 0.9 tuned as per the settling voltage at the output terminals of SZSC [16]. With the given MFs and ranges, 49 IF-AND-IF-THEN rules are set in the rule editor of the FIS tool as per the given rule in Table 1.

After updating the rules, the FIS file is exported to the 'workspace' of MATLAB software, which is called into the simulation. The output variable 'D' is generated as per the ranges and rules set in the FIS tool.

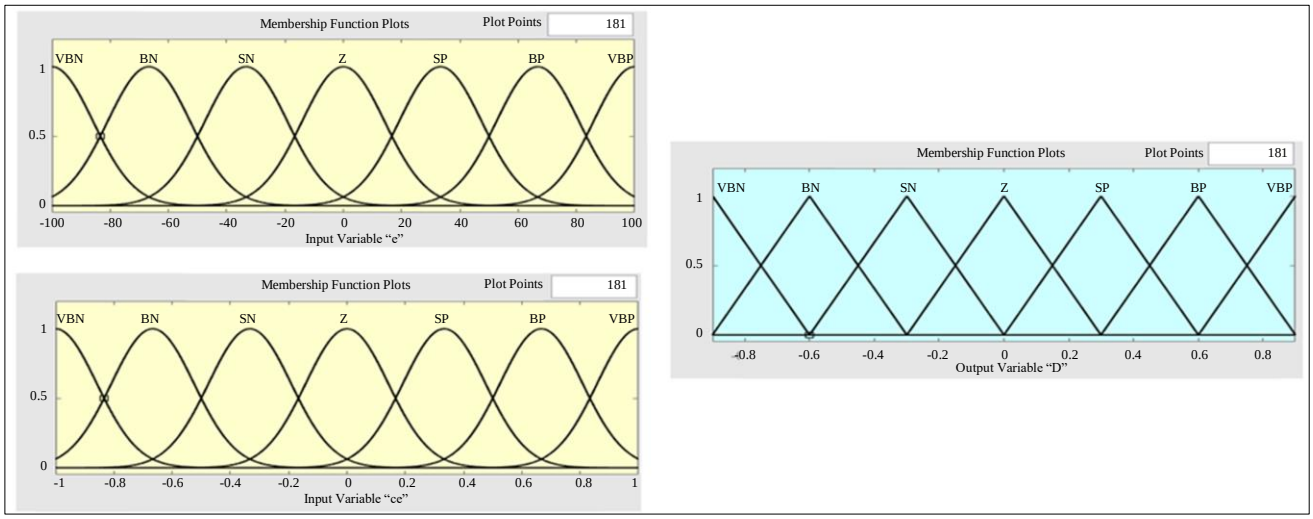

Fig. 4 MFs of input and output variables of FIS

Table 1. Rule table

D	**'e'**							
'ce'		**VBN**	**BN**	**SN**	**Z**	**SP**	**BP**	**VBP**
	VBN	VBN	VBN	VBN	VBN	BN	SN	Z
	BN	VBN	VBN	VBN	BN	SN	Z	SP
	SN	VBN	VBN	BN	SN	Z	SP	BP
	Z	VBN	BN	SN	Z	SP	BP	VBP
	SP	BN	SN	Z	SP	BP	VBP	VBP
	BP	SN	Z	SP	BP	VBP	VBP	VBP
	VBP	Z	SP	BP	VBP	VBP	VBP	VBP

3. Switched Capacitor Multi Level Inverter (SC-MLI) Design

For converting DC to three phase AC voltages with multiple voltage levels replicating a Sin wave, a SC-MLI circuit topology is adopted. The proposed SC-MLI topology is a unique MLI which needs only one DC source at the input. Most of the MLI topologies, like diode clamp, cascaded H-bridge, and asymmetrical MLI, need multiple sources either with the same or different voltage levels [17]. In the proposed circuit structure, the output from the SZSC is considered to be a single DC source with accumulated renewable power. Therefore, the only option for generating multi-level AC voltages is connecting a SC-MLI at the output of SZSC. The proposed SC-MLI generates a 9-level AC voltage in each phase operated by the PWM technique [18]. The circuit structure of the 9-level SC-MLI of one phase is presented in Figure 5.

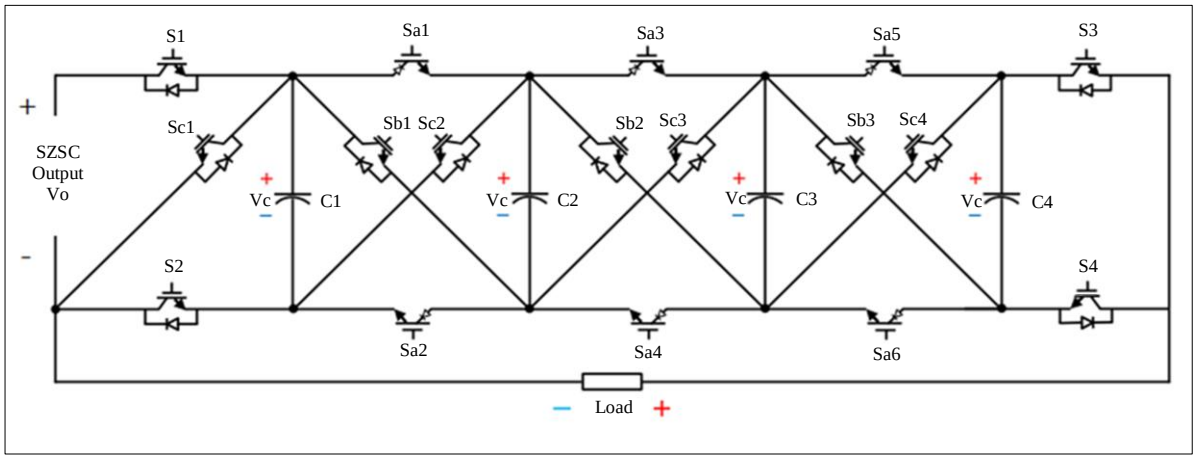

Fig. 5 Circuit structure of 9-level SC-MLI

As observed in Figure 5, the topology contains four voltage dividing capacitors (C_1 – C_4), eleven IGBT – Diode switches (S_1 – S_4, S_{b1} – S_{b3}, S_{c1} – S_{c4}) and six IGBT switches (S_{a1} – S_{a6}). The IGBT – Diode and IGBT switches are controlled using PWM pulses generated by comparison of four level shifted high frequency triangular waveforms with fundamental frequency reference signal [19]. The fundamental frequency reference signal is generated by a space vector reference generator producing SV-PWM pulses for the SC-MLI. Figure 6 represents the comparison of SV signal with triangular waveforms for controlling the switches of SC-MLI [20].

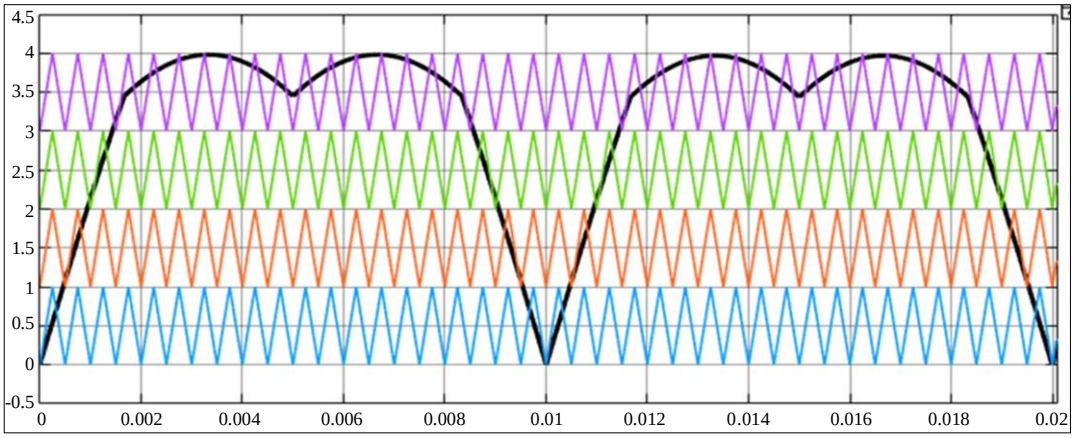

Fig. 6 SV-PWM pulse generation for SC-MLI

As seen in Figure 6, the reference waveform is the third harmonic content signal generated with respect to the sector selection in the space vector generator. These space vector reference signals are generated by reference Sin signals with synchronized amplitude, frequency and phase of the three-phase grid. There are generally eight vectors in SV-PWM in which two vectors are considered to be zero voltage vectors, are no voltage is generated during these states. The remaining six vectors create positive and negative AC voltage for the three phases of the SC-MLI. The hexagon vector generation by the space vector technique is presented in Figure 7.

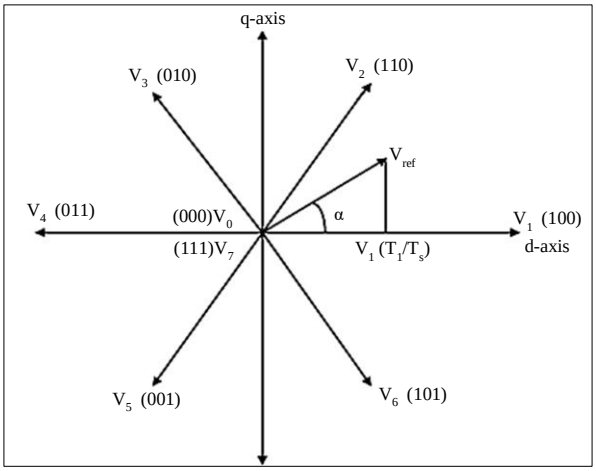

Fig. 7 Vector diagram of the space vector technique

In Figure 7, 'α' is the angle of the reference Sin signal taken from the grid voltages. As per the 'α' angle of the voltage sector selection is considered. The 'β' voltage vector is always in 90 degree phase lag shift to the 'α' angle [21]. For the three-phase voltage, there are three dwell times (T_a T_b T_0) to create the reference space vector signals calculated as:

$$T_a = m \frac{Sin\left(\frac{\pi}{3}-\alpha\right)}{Sin\left(\frac{\pi}{3}\right)} T_s \quad (7)$$

$$T_b = m \frac{Sin(\alpha)}{Sin\left(\frac{\pi}{3}\right)} T_s \quad (8)$$

$$T_0 = \frac{T_s - T_a - T_b}{2} \quad (9)$$

Here, m is the magnitude of the voltage per unit, and T_s is taken as $1/f_s$ (f_s = switching frequency). As per the dwell times (T_a T_b T_0), the space vector reference signals ($V_{ref\_a}V_{ref\_b}V_{ref\_c}$)are generated with respect to the vector in Figure 7 presented in Table 2 [21].

All the modules (sources, SZSC and SC-MLI) are modelled as per the given configuration and mathematical expressions, creating a test system for analysis. The next section gives a brief detail on the modeling simulation of the proposed test system with results and analysis.

Table 2. Vector selection table

Vector	Phase-A (V_{ref_a})	Phase-B (V_{ref_b})	Phase-C (V_{ref_c})
1	Ta + Tb + T0	Tb + T0	T0
2	Ta + T0	Ta + Tb + T0	T0
3	T0	Ta + Tb + T0	Tb + T0
4	T0	Ta + T0	Ta + Tb + T0
5	Tb + T0	T0	Ta + Tb + T0
6	Ta + Tb + T0	T0	Ta + T0

4. Simulation Results

The modeling of renewable sources (PV panels and wind turbine generator) with energy storage module support, SZSC and SC-MLI with grid interconnection is done in the Simulink environment. All the blocks for the modeling of the mentioned modules are taken from the 'Specialized technology' of the 'Power systems' block set in the library browser. Blocks from 'Commonly used blocks' of the 'Simulink' subset are also considered for measurements graphical representation. Each and every block is updated with specifications as per the requirement of the standard electrical system given in Table 3.

Table 3. System specifications

Name of the Module	Parameters
PV Unit	PVA: PVA: Vmp = 13.6V, Imp = 5.46A, Voc = 16.1V, Isc = 6.05A, Ns = 1, Np = 9, Ppv = 735W. Boost converter: Lb = 1.2mH, Cin = 120µF. Rigbt = 0.1mΩ, fs = 5000Hz.
Wind Farm Unit	PMSG: 6Nm 310Vdc 4600rpm, Rs = 0.61Ω, Ls = 2.061mH, φ = 0.08618V.sBuck-Boost converter: L_{bbc} = 120µH, R_{igbt} = 0.1mΩ, f_s = 5kHz.
Battery Unit	Battery: Vnom = 12.4V, Capacity = 43Ahr. Bidirectional Converter: Lbdc = 151.45µH, Cout = 10mF, Rigbt = 0.1mΩ, fs = 5kHz
SZSC	L1 = L2 = 320µH, C1 = C2 = C3 = 390µF, Rmosfet = 0.01Ω, Cdc = 1100µF, Vdc ref = 100V, Kp = 0.055, Ki = 0.0025, fs = 5kHz
MLI	Vin = 100Vdc, Vac L = 400Vac rms, fs = 2000Hz, Rigbt = 0.1mΩ, C1 = C2 = C3 = C4 = 1.2mF. Lf = 580µH, Cf = 120µF.
Grid	400$V_{rms\ ph\text{-}ph}$ 50Hz
Load	500W 400$V_{rms\ ph\text{-}ph}$ 50Hz

As per the given parameters the models are updated with the same rating of the sources, circuits and loads connected to the grid. The simulation is run for 3sec with different operating conditions set for PV sources and wind farms. The solar irradiation is set at 1000W/m2 initially, which is later dropped to 500W/m2 at 2sec and the wind speed is set at 12m/s initially later dropped to 8m/s at 1sec. The load is always fixed at 500W, which is compensated by either renewable modules or the grid.

The first model is run with Quasi Z Source Converter (QZSC) at the DC link, and a six-switch Voltage Source Inverter (VSI) for AC voltage generation interconnected to the grid through the LC filter. This model is considered as conventional topology with low gain, high ripple and high

harmonic content. To overcome these issues the conventional QZSC is replaced with SZSC with high gain and reduced ripple DC voltage capabilities.

The six-switch converter is replaced with three phase 9-level SC-MLI for reduced harmonic voltages. The SZSC MOSFET switch is controlled by a PI voltage regulator set with a 100V reference. The three phase 9-level SC-MLI is controlled by a novel Sin PWM technique synchronized to the grid three phase voltages. The graphs of powers, voltages and currents of all the modules are plotted with respect to time and are presented below.

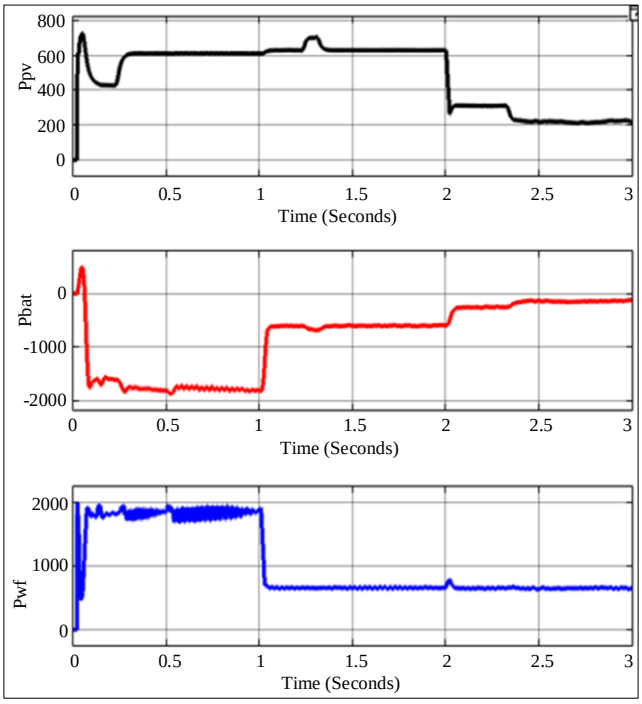

Fig. 8 Active powers of PV panels, wind turbine generator and battery

Figure 8 represents the active powers of the PV panels, battery module and wind turbine generator. The Ppv initially is 600W from 0 – 2sec and reduced to 200W at 2sec due to a drop in solar irradiation until 3sec. The wind turbine generator initially generates 2000W from 0 – 1 sec, which drops to 700W at 1 sec due to a drop in wind speed until 3 sec. The battery stores 2000W from 0 – 1sec and reduces to 700W storage from 1 – 2sec and later with no exchange of power from 2 – 3 sec.

Figure 9 shows the graphs of input power from renewable sources, the output power of the inverter and the total power loss of the complete system. The input power from renewable sources is recorded at 700W, shared by the PV panel and wind turbine generator. The received power at the inverter side is 500W with conversion and switching losses of 200W. The input and output voltage of the SZSC are presented in Figure 10.

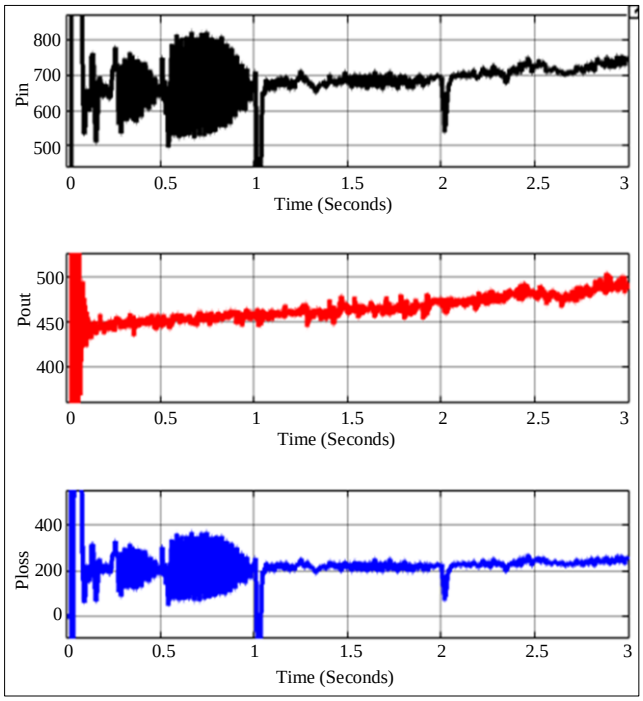

Fig. 9 Input, output and loss of active powers of the system

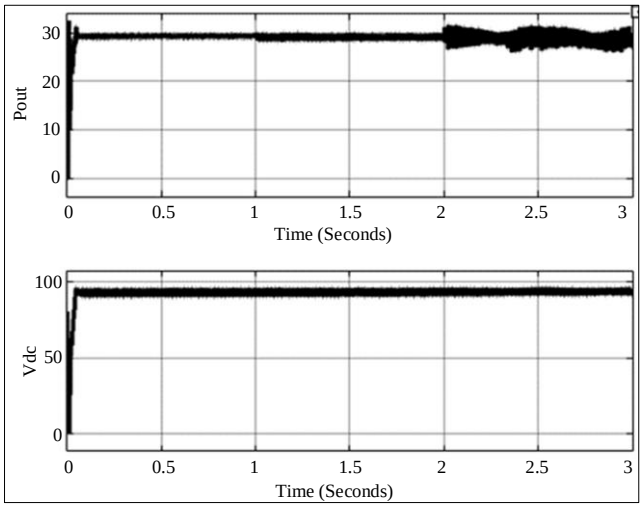

Fig. 10 Input and output DC voltage of SZSC

The input voltage to the SZSC is noted to be 30V, which is boosted to 100V by the SZSC voltage regulator. As per the 100Vdc voltage generated by the SZSC, the SC-MLI 9-level voltages are presented in Figure 11. Figure 11(a) is the three phase 9-level AC voltages generated by the SC-MLI with an amplitude of 400V. The three phase AC voltages after the LC filter connected at the output of the SC-MLI are presented in Figure 11(b). In Figure 12, the active powers of the renewable sources, grid and load are presented.

The active power shared by the renewable sources is noted to be 500W, compensating the load of 500W. The deficit power during the initial simulation is compensated by the grid

maintaining the load power stable at 500W. The SZSC controller is updated with the FIS voltage regulator generating duty ratio to the MOSFET switch presented in the rule viewer of Figure 13.

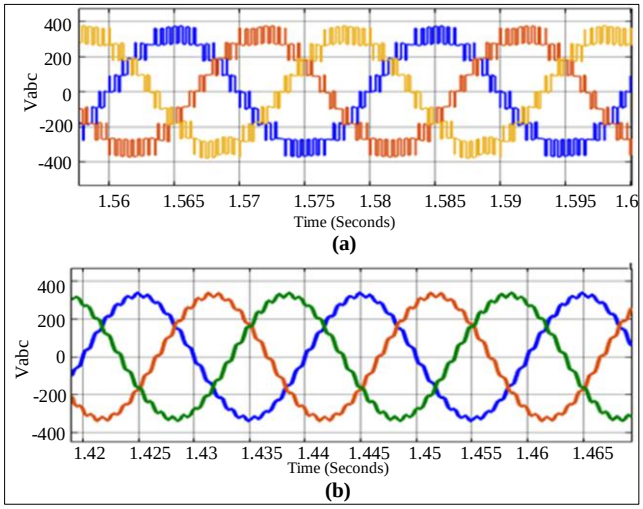

Fig. 11 Three phase voltage of SC-MLI (a) Before LC filter, and (b) After LC filter.

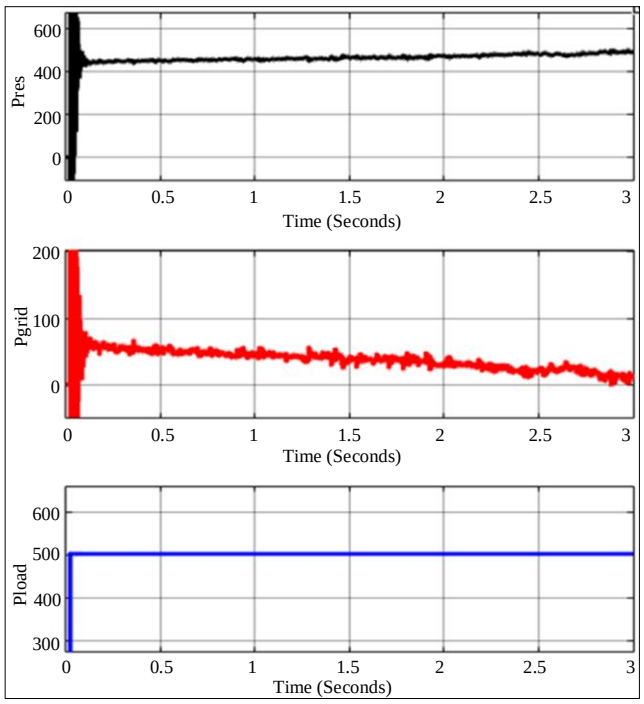

Fig. 12 Active powers of renewable sources, grid and load

The duty ratio for the MOSFET is estimated as per the 'e' and 'ce' values input given to the FIS voltage regulator. As per the updated FIS voltage regulator, the DC voltage stability and magnitude are increased as compared to the traditional PI voltage regulator. The Sin reference input is replaced with an SV signal generator as per the sector generation with respect to the phase angle of the grid phase A voltage shown in Figure 14. The sector continuously varies from 1 – 6 for each cycle of the AC voltage generating reference SV signals to the SC-MLI PWM generator. With the updates to the DC voltage regulator and SC-MLI control, comparative graphs of SZSC output voltage and inverter output powers are presented in Figures 15 and 16.

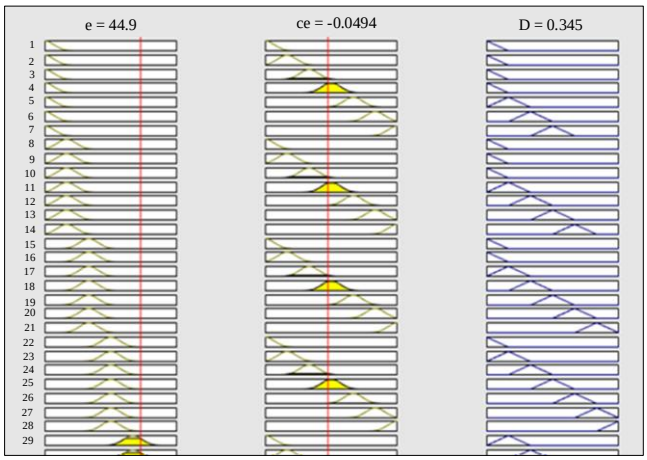

Fig. 13 FIS voltage regulator rule viewer

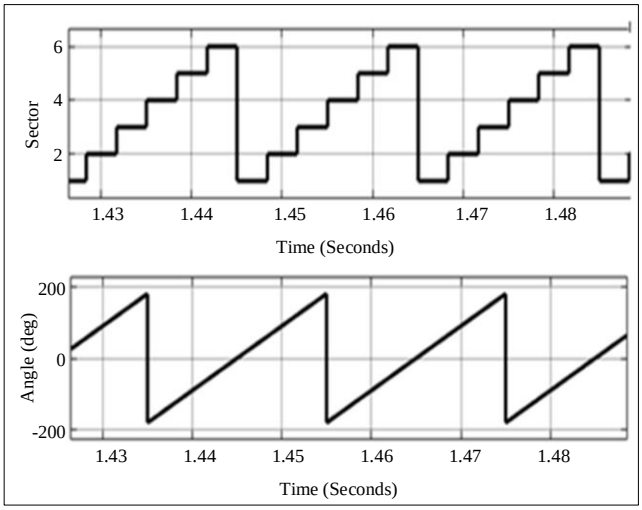

Fig. 14 Grid voltage angle and sector in SV signal generator

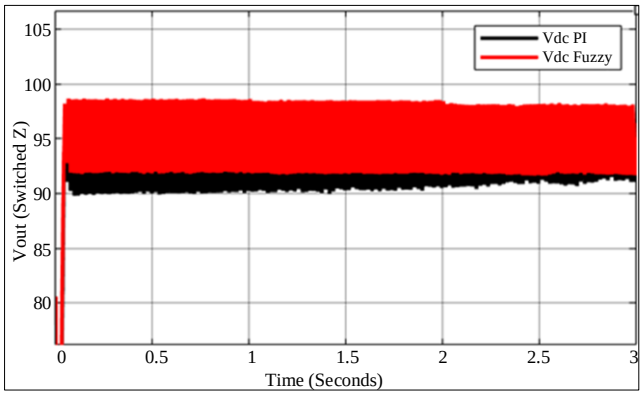

Fig. 15 DC link voltage comparison

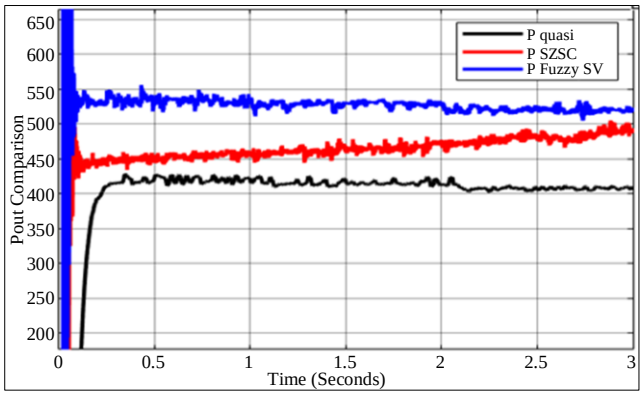

Fig. 16 Inverter output power comparison

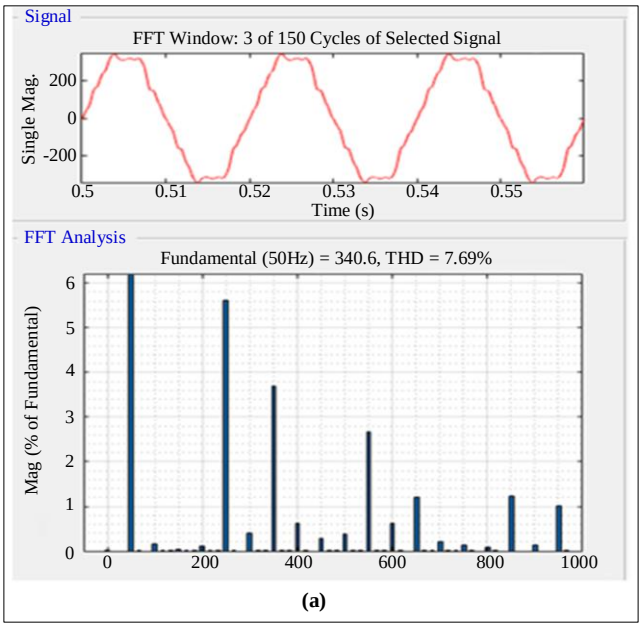

(a)

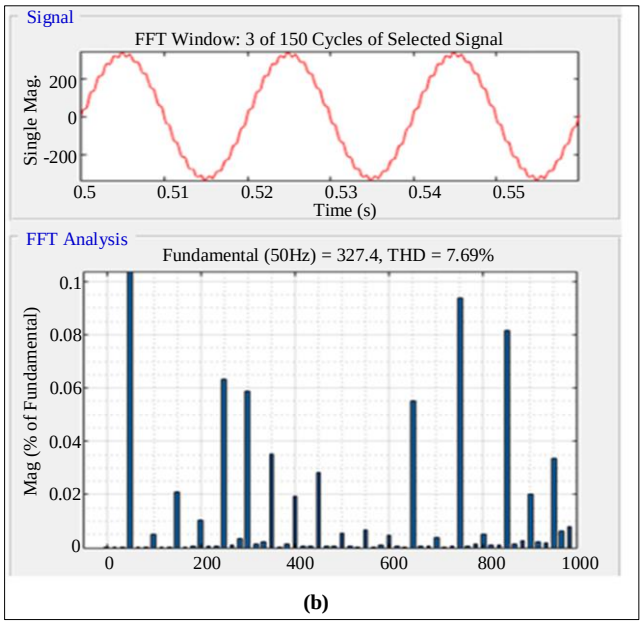

(b)

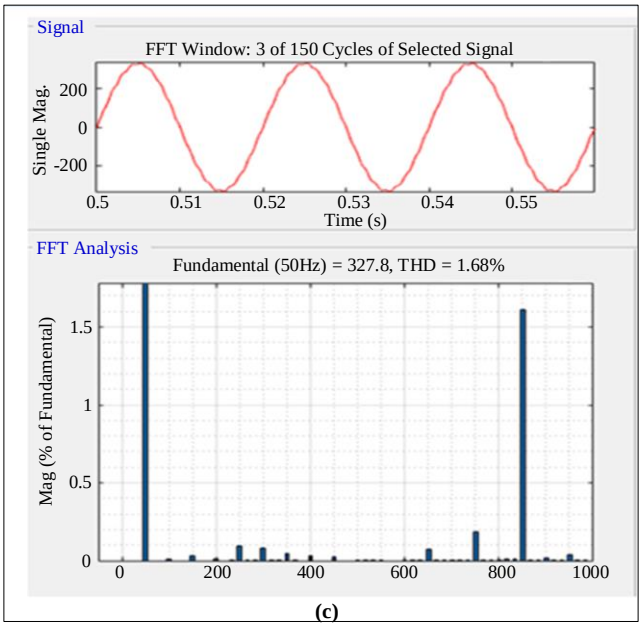

(c)

Fig. 17 Phase A voltage THDs of (a) QZSC six switch inverter, (b) SZSC PI regulator and SC-MLI Sin-PWM, and (c) SZSC FIS regulator and SC-MLI SV-PWM.

It is observed that there is an increase in DC voltage magnitude and stability when the SZSC is operated with an FIS voltage regulator. This improves the stability even in the AC voltages, leading to reduced harmonics. As per Figure 16, it is noticed that the power shared by the inverter with SV SC-MLI control has a higher magnitude as compared to conventional models.

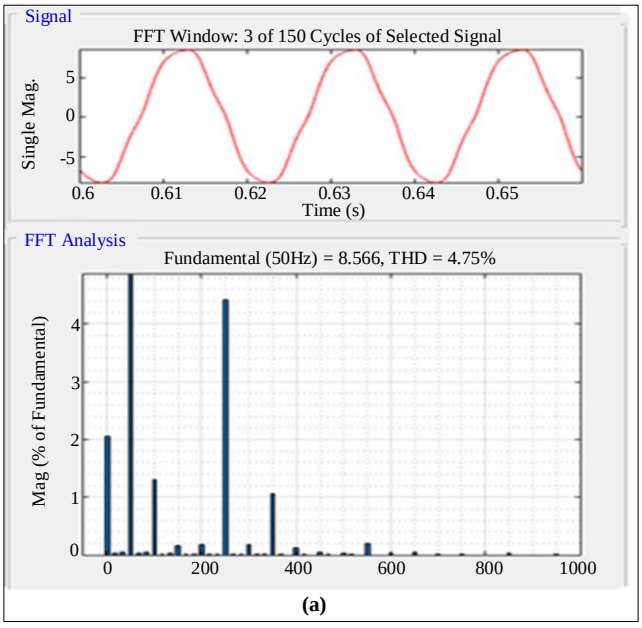

(a)

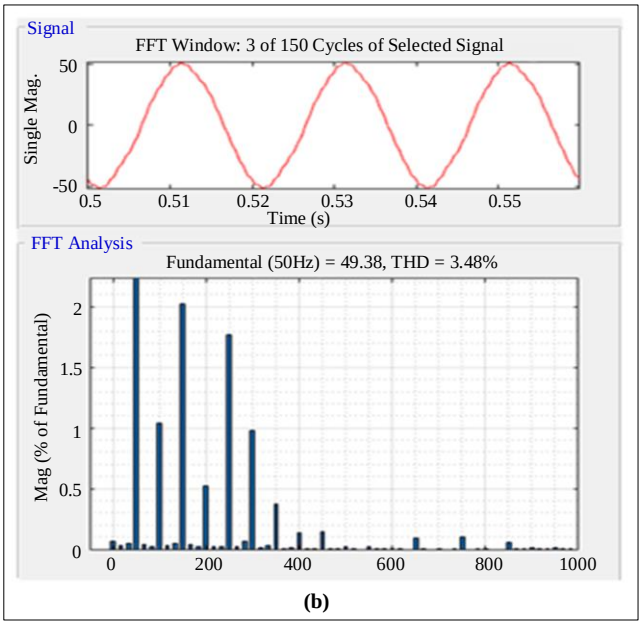

(b)

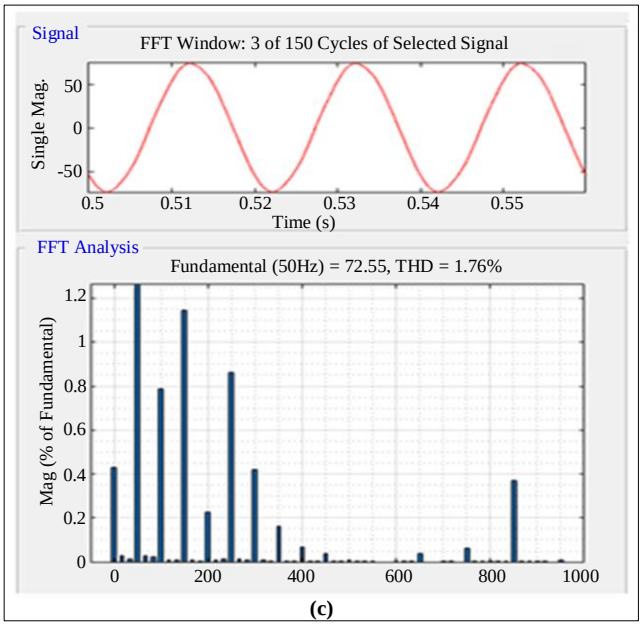

(c)

Fig. 18 Phase A Current THDs of (a) QZSC six switch inverter, (b) SZSC PI regulator and SC-MLI Sin-PWM, and (c) SZSC PI regulator and SC-MLI SV-PWM.

As per the FFT analysis of the inverter voltage and current of the different topologies, it is observed that the THD is lesser for the model with an FIS voltage regulator and SV-PWM technique. The QZSC six switch inverter records high harmonic content, which is reduced by the SZSC SC-MLI topology. A comparative Table 4 is presented with values taken from the FFT analysis tool of the Simulink models.

Table 4. Comparison table

Name of the Parameter	QZSC Six Switch	SZSC PI, SC-MLI Sin PWM	SZSC FIS, SC-MLI SV-PWM
THD of voltage	7.69%	3.84%	1.68%
THD of current	4.75%	3.48%	1.76%

5. Conclusion

Different topologies sharing renewable power at low rating voltages and powers are proposed with circuit structure design and modeling. The capability of the SZSC over the QZSC with high gain voltage boosting is presented. Replacement of conventional six switch topology with SC-MLI achieves lower harmonic content in the AC voltage, stabilizing the voltages on the load side.

Efficient power sharing from the lower voltage level renewable sources in the range of 30V is achieved. A magnitude of approximately 400V AC voltage is generated at the SC-MLI with input voltages of 30V showing a voltage gain of 13 times. This high range gain demonstrates the performance of the system when operated with lower rating renewable sources.

The converter's performance is further improved when the PI voltage regulator is replaced with the FIS voltage regulator, and Sin-PWM is replaced by SV-PWM. With these updates, the DC voltage stability is achieved along with reduced harmonic content in the AC voltages. The active power shared by the system with new controller modules is increased by 10%, validating the performance of the proposed system.

References

[1] Glen G. Farivar et al., "Grid-Connected Energy Storage Systems: State-of-the-Art and Emerging Technologies," *Proceedings of the IEEE*, vol. 111, no. 4, pp. 397-420, 2023. [CrossRef] [Google Scholar] [Publisher Link]

[2] Shimaa Barakat, A. Emam, and M.M. Samy, "Investigating Grid-Connected Green Power Systems'energy Storage Solutions in the Event of Frequent Blackouts," *Energy Reports*, vol. 8, pp. 5177-5191, 2022. [CrossRef] [Google Scholar] [Publisher Link]

[3] P. Padamanabhan, and R. Sharma, "Renewable Energy Storage Systems with Grid Connected Solar Using Multi-Objective Optimization Technique," *2nd International Conference for Innovation in Technology (INOCON)*, Bangalore, India, pp. 1-7, 2023. [CrossRef] [Google Scholar] [Publisher Link]

[4] Jesus C. Hernandez, "Grid-Connected Renewable Energy Sources", *Electronics*, vol. 10, no. 5, 2021. [CrossRef] [Publisher Link]

[5] Junfeng Liu et al., "Switched Z-Source/Quasi-Z-Source DC-DC Converters with Reduced Passive Components for Photovoltaic Systems," *IEEE Access*, vol. 7, pp. 40893-40903, 2019. [CrossRef] [Google Scholar] [Publisher Link]

[6] Mehdi Samizadeh et al., "A New Topology of Switched-Capacitor Multilevel Inverter with Eliminating Leakage Current," *IEEE Access*, vol. 8, pp. 76951-76965, 2020. [CrossRef] [Google Scholar] [Publisher Link]

[7] Habib Ur Rahman Habib, Shaorong Wang, and Muhammad Tajamul Aziz, "PV-Wind-Battery Based Standalone Microgrid System with MPPT for Green and Sustainable Future," *9th International Conference on Power and Energy Systems (ICPES)*, Perth, WA, Australia, pp. 1-6, 2019. [CrossRef] [Google Scholar] [Publisher Link]

[8] Muhammad Maaruf, Khalid Khan, and Muhammad Khalid, "Robust Control for Optimized Islanded and Grid-Connected Operation of Solar/Wind/Battery Hybrid Energy," *Sustainability*, vol. 14, no. 9, 2022. [CrossRef] [Google Scholar] [Publisher Link]

[9] Somnath Das, and Ashok Kumar Akella, "Power Flow Control of PV-Wind-Battery Hybrid Renewable Energy Systems for Stand-Alone Application," *International Journal of Renewable Energy Research*, vol. 8, no. 1, pp. 36-43, 2018. [CrossRef] [Google Scholar] [Publisher Link]

[10] N.F. Nik Ismail et al., "Fuzzy Logic Controller on DC/DC Boost Converter," *IEEE International Conference on Power and Energy*, Kuala Lumpur, Malaysia, pp. 661-666, 2010. [CrossRef] [Google Scholar] [Publisher Link]

[11] Mohammad Mehdi Haji-Esmaeili, Ebrahim Babaei, and Mehran Sabahi, "High Step-Up Quasi-Z Source DC-DC Converter," *IEEE Transactions on Power Electronics*, vol. 33, no. 12, pp. 10563-10571, 2018. [CrossRef] [Google Scholar] [Publisher Link]

[12] Guidong Zhang et al., ''An Impedance Network Boost Converter with a High-Voltage Gain," *IEEE Transactions on Power Electronics*, vol. 32, no. 9, pp. 6661-6665, 2017. [CrossRef] [Google Scholar] [Publisher Link]

[13] Nadeem Javaid et al., "An Intelligent Load Management System with Renewable Energy Integration for Smart Homes," *IEEE Access*, vol. 5, pp. 13587-13600, 2017. [CrossRef] [Google Scholar] [Publisher Link]

[14] Bhim Singh, and Vashist Bist, "A Single Sensor Based PFC Zeta Converter Fed BLDC Motor Drive for Fan Applications," *IEEE Fifth Power India Conference*, Murthal, India, pp. 1-6, 2012. [CrossRef] [Google Scholar] [Publisher Link]

[15] Ying Zhu, Zhengzhou Ma, and Zhicong Wang, "An Improved Fuzzy Logic Based DC-Link Voltage Control Strategy for Smoothing Output Power of the PMSG-WECS," *Energy Reports*, vol. 8, pp. 8413-8425, 2022. [CrossRef] [Google Scholar] [Publisher Link]

[16] Ajay Dheeraj, and Afzal Sikander, "Fuzzy Logic Based Control of Voltage and Transient Stability in a DC Microgrid," *2nd International Conference for Emerging Technology (INCET)*, Belagavi, India, pp. 1-6, 2021. [CrossRef] [Google Scholar] [Publisher Link]

[17] Reza Barzegarkhoo et al., "A New Boost Switched-Capacitor Multilevel Converter with Reduced Circuit Devices," *IEEE Transactions on Power Electronics*, vol. 33, no. 8, pp. 6738-6754, 2018. [CrossRef] [Google Scholar] [Publisher Link]

[18] Venu Sonti, Sachin Jain, and Subhashish Bhattacharya, "Analysis of the Modulation Strategy for the Minimization of the Leakage Current in the PV Grid-Connected Cascaded Multilevel Inverter," *IEEE Transactions on Power Electronics*, vol. 32, no. 2, pp. 1156-1169, 2017. [CrossRef] [Google Scholar] [Publisher Link]

[19] Mehdi Samizadeh et al., "A New Topology of Switched-Capacitor Multilevel Inverter for Single-Phase Grid-Connected with Eliminating Leakage Current," *International Power Electronics Conference (IPEC-Niigata 2018 -ECCE Asia)*, Niigata, Japan, pp. 2854-2859, 2018. [CrossRef] [Google Scholar] [Publisher Link]

[20] Qamar Muhammad Attique, Yongdong Li, and Kui Wang, "A Survey on Space-Vector Pulse Width Modulation for Multilevel Inverters," *CPSS Transactions on Power Electronics and Applications*, vol. 2, no. 3, pp. 226-236, 2017. [CrossRef] [Google Scholar] [Publisher Link]

[21] A.C. Binojkumar, B. Saritha, and G. Narayanan, "Experimental Comparison of Conventional and Bus-Clamping PWM Methods Based on Electrical and Acoustic Noise Spectra of Induction Motor Drives", *IEEE Transactions on Industry Applications*, vol. 52, no. 5, pp. 4061-4073, 2016. [CrossRef] [Google Scholar] [Publisher Link]